BELLE-CONF-0455
ICHEP04 11-0703

Search for $D^0 - \overline{D^0}$ mixing using semileptonic decays at Belle

K. Abe,[10] K. Abe,[46] N. Abe,[49] I. Adachi,[10] H. Aihara,[48] M. Akatsu,[24] Y. Asano,[53] T. Aso,[52] V. Aulchenko,[2] T. Aushev,[14] T. Aziz,[44] S. Bahinipati,[6] A. M. Bakich,[43] Y. Ban,[36] M. Barbero,[9] A. Bay,[20] I. Bedny,[2] U. Bitenc,[15] I. Bizjak,[15] S. Blyth,[29] A. Bondar,[2] A. Bozek,[30] M. Bračko,[22,15] J. Brodzicka,[30] T. E. Browder,[9] M.-C. Chang,[29] P. Chang,[29] Y. Chao,[29] A. Chen,[26] K.-F. Chen,[29] W. T. Chen,[26] B. G. Cheon,[4] R. Chistov,[14] S.-K. Choi,[8] Y. Choi,[42] Y. K. Choi,[42] A. Chuvikov,[37] S. Cole,[43] M. Danilov,[14] M. Dash,[55] L. Y. Dong,[12] R. Dowd,[23] J. Dragic,[23] A. Drutskoy,[6] S. Eidelman,[2] Y. Enari,[24] D. Epifanov,[2] C. W. Everton,[23] F. Fang,[9] S. Fratina,[15] H. Fujii,[10] N. Gabyshev,[2] A. Garmash,[37] T. Gershon,[10] A. Go,[26] G. Gokhroo,[44] B. Golob,[21,15] M. Grosse Perdekamp,[38] H. Guler,[9] J. Haba,[10] F. Handa,[47] K. Hara,[10] T. Hara,[34] N. C. Hastings,[10] K. Hasuko,[38] K. Hayasaka,[24] H. Hayashii,[25] M. Hazumi,[10] E. M. Heenan,[23] I. Higuchi,[47] T. Higuchi,[10] L. Hinz,[20] T. Hojo,[34] T. Hokuue,[24] Y. Hoshi,[46] K. Hoshina,[51] S. Hou,[26] W.-S. Hou,[29] Y. B. Hsiung,[29] H.-C. Huang,[29] T. Igaki,[24] Y. Igarashi,[10] T. Iijima,[24] A. Imoto,[25] K. Inami,[24] A. Ishikawa,[10] H. Ishino,[49] K. Itoh,[48] R. Itoh,[10] M. Iwamoto,[3] M. Iwasaki,[48] Y. Iwasaki,[10] R. Kagan,[14] H. Kakuno,[48] J. H. Kang,[56] J. S. Kang,[17] P. Kapusta,[30] S. U. Kataoka,[25] N. Katayama,[10] H. Kawai,[3] H. Kawai,[48] Y. Kawakami,[24] N. Kawamura,[1] T. Kawasaki,[32] N. Kent,[9] H. R. Khan,[49] A. Kibayashi,[49] H. Kichimi,[10] H. J. Kim,[19] H. O. Kim,[42] Hyunwoo Kim,[17] J. H. Kim,[42] S. K. Kim,[41] T. H. Kim,[56] K. Kinoshita,[6] P. Koppenburg,[10] S. Korpar,[22,15] P. Križan,[21,15] P. Krokovny,[2] R. Kulasiri,[6] C. C. Kuo,[26] H. Kurashiro,[49] E. Kurihara,[3] A. Kusaka,[48] A. Kuzmin,[2] Y.-J. Kwon,[56] J. S. Lange,[7] G. Leder,[13] S. E. Lee,[41] S. H. Lee,[41] Y.-J. Lee,[29] T. Lesiak,[30] J. Li,[40] A. Limosani,[23] S.-W. Lin,[29] D. Liventsev,[14] J. MacNaughton,[13] G. Majumder,[44] F. Mandl,[13] D. Marlow,[37] T. Matsuishi,[24] H. Matsumoto,[32] S. Matsumoto,[5] T. Matsumoto,[50] A. Matyja,[30] Y. Mikami,[47] W. Mitaroff,[13] K. Miyabayashi,[25] Y. Miyabayashi,[24] H. Miyake,[34] H. Miyata,[32] R. Mizuk,[14] D. Mohapatra,[55] G. R. Moloney,[23] G. F. Moorhead,[23] T. Mori,[49] A. Murakami,[39] T. Nagamine,[47] Y. Nagasaka,[11] T. Nakadaira,[48] I. Nakamura,[10] E. Nakano,[33] M. Nakao,[10] H. Nakazawa,[10] Z. Natkaniec,[30] K. Neichi,[46] S. Nishida,[10] O. Nitoh,[51] S. Noguchi,[25] T. Nozaki,[10] A. Ogawa,[38] S. Ogawa,[45] T. Ohshima,[24] T. Okabe,[24] S. Okuno,[16] S. L. Olsen,[9] Y. Onuki,[32] W. Ostrowicz,[30] H. Ozaki,[10] P. Pakhlov,[14] H. Palka,[30] C. W. Park,[42] H. Park,[19] K. S. Park,[42] N. Parslow,[43] L. S. Peak,[43] M. Pernicka,[13] J.-P. Perroud,[20] M. Peters,[9] L. E. Piilonen,[55] A. Poluektov,[2] F. J. Ronga,[10] N. Root,[2] M. Rozanska,[30] H. Sagawa,[10] M. Saigo,[47] S. Saitoh,[10] Y. Sakai,[10] H. Sakamoto,[18] T. R. Sarangi,[10] M. Satapathy,[54] N. Sato,[24] O. Schneider,[20] J. Schümann,[29] C. Schwanda,[13] A. J. Schwartz,[6] T. Seki,[50] S. Semenov,[14] K. Senyo,[24] Y. Settai,[5] R. Seuster,[9] M. E. Sevior,[23] T. Shibata,[32] H. Shibuya,[45] B. Shwartz,[2] V. Sidorov,[2] V. Siegle,[38] J. B. Singh,[35] A. Somov,[6] N. Soni,[35] R. Stamen,[10] S. Stanič,[53,*] M. Starič,[15] A. Sugi,[24] A. Sugiyama,[39] K. Sumisawa,[34] T. Sumiyoshi,[50] S. Suzuki,[39] S. Y. Suzuki,[10] O. Tajima,[10] F. Takasaki,[10] K. Tamai,[10] N. Tamura,[32] K. Tanabe,[48] M. Tanaka,[10] G. N. Taylor,[23] Y. Teramoto,[33] X. C. Tian,[36] S. Tokuda,[24] S. N. Tovey,[23] K. Trabelsi,[9] T. Tsuboyama,[10]

T. Tsukamoto,[10] K. Uchida,[9] S. Uehara,[10] T. Uglov,[14] K. Ueno,[29] Y. Unno,[3] S. Uno,[10] Y. Ushiroda,[10] G. Varner,[9] K. E. Varvell,[43] S. Villa,[20] C. C. Wang,[29] C. H. Wang,[28] J. G. Wang,[55] M.-Z. Wang,[29] M. Watanabe,[32] Y. Watanabe,[49] L. Widhalm,[13] Q. L. Xie,[12] B. D. Yabsley,[55] A. Yamaguchi,[47] H. Yamamoto,[47] S. Yamamoto,[50] T. Yamanaka,[34] Y. Yamashita,[31] M. Yamauchi,[10] Heyoung Yang,[41] P. Yeh,[29] J. Ying,[36] K. Yoshida,[24] Y. Yuan,[12] Y. Yusa,[47] H. Yuta,[1] S. L. Zang,[12] C. C. Zhang,[12] J. Zhang,[10] L. M. Zhang,[40] Z. P. Zhang,[40] V. Zhilich,[2] T. Ziegler,[37] D. Žontar,[21,15] and D. Zürcher[20]

(The Belle Collaboration)

[1]*Aomori University, Aomori*
[2]*Budker Institute of Nuclear Physics, Novosibirsk*
[3]*Chiba University, Chiba*
[4]*Chonnam National University, Kwangju*
[5]*Chuo University, Tokyo*
[6]*University of Cincinnati, Cincinnati, Ohio 45221*
[7]*University of Frankfurt, Frankfurt*
[8]*Gyeongsang National University, Chinju*
[9]*University of Hawaii, Honolulu, Hawaii 96822*
[10]*High Energy Accelerator Research Organization (KEK), Tsukuba*
[11]*Hiroshima Institute of Technology, Hiroshima*
[12]*Institute of High Energy Physics, Chinese Academy of Sciences, Beijing*
[13]*Institute of High Energy Physics, Vienna*
[14]*Institute for Theoretical and Experimental Physics, Moscow*
[15]*J. Stefan Institute, Ljubljana*
[16]*Kanagawa University, Yokohama*
[17]*Korea University, Seoul*
[18]*Kyoto University, Kyoto*
[19]*Kyungpook National University, Taegu*
[20]*Swiss Federal Institute of Technology of Lausanne, EPFL, Lausanne*
[21]*University of Ljubljana, Ljubljana*
[22]*University of Maribor, Maribor*
[23]*University of Melbourne, Victoria*
[24]*Nagoya University, Nagoya*
[25]*Nara Women's University, Nara*
[26]*National Central University, Chung-li*
[27]*National Kaohsiung Normal University, Kaohsiung*
[28]*National United University, Miao Li*
[29]*Department of Physics, National Taiwan University, Taipei*
[30]*H. Niewodniczanski Institute of Nuclear Physics, Krakow*
[31]*Nihon Dental College, Niigata*
[32]*Niigata University, Niigata*
[33]*Osaka City University, Osaka*
[34]*Osaka University, Osaka*
[35]*Panjab University, Chandigarh*
[36]*Peking University, Beijing*
[37]*Princeton University, Princeton, New Jersey 08545*

[38]RIKEN BNL Research Center, Upton, New York 11973
[39]Saga University, Saga
[40]University of Science and Technology of China, Hefei
[41]Seoul National University, Seoul
[42]Sungkyunkwan University, Suwon
[43]University of Sydney, Sydney NSW
[44]Tata Institute of Fundamental Research, Bombay
[45]Toho University, Funabashi
[46]Tohoku Gakuin University, Tagajo
[47]Tohoku University, Sendai
[48]Department of Physics, University of Tokyo, Tokyo
[49]Tokyo Institute of Technology, Tokyo
[50]Tokyo Metropolitan University, Tokyo
[51]Tokyo University of Agriculture and Technology, Tokyo
[52]Toyama National College of Maritime Technology, Toyama
[53]University of Tsukuba, Tsukuba
[54]Utkal University, Bhubaneswer
[55]Virginia Polytechnic Institute and State University, Blacksburg, Virginia 24061
[56]Yonsei University, Seoul

Abstract

A search for mixing in the neutral D meson system was performed using semileptonic $D^0 \to K^- e^+ \nu$ decays. The flavor of neutral D mesons at production was tagged by the charge of the slow pion from the decay $D^{*+} \to D^0 \pi^+$. The measurement was performed using 140 fb^{-1} of data recorded by the Belle detector. The yield of right and wrong sign decays arising from un-mixed and mixed events, respectively, was determined by a fit to kinematic observables. From the number of signal events we derive an upper limit for the time-integrated mixing rate $r_D < 1.4 \times 10^{-3}$ at 90% C.L.

PACS numbers: 13.20.Fc, 14.40.Lb

I INTRODUCTION

By considering the quark box diagrams describing $D^0 - \overline{D}^0$ mixing (Fig.1), it is easy to see why the mixing rate in the charm sector is expected to be small. The amplitude for

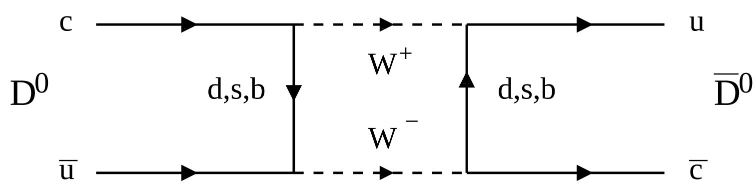

FIG. 1: Box diagram for the D^0 mixing amplitude.

these processes can be written as

$$< \overline{D}^0 | H_{\mathrm{weak}} | D^0 > \quad \propto \sum_{i,j=d,s,b} V_{ci}^* V_{ui} V_{cj} V_{uj}^* \ \mathcal{K}(m_i^2, m_j^2) \quad , \tag{1}$$

where V_{kl} are the Cabibbo-Kobayashi-Maskawa (CKM) matrix elements [1] and $\mathcal{K}$ is the loop function depending on the masses of down-like quarks. The contribution of b quarks is negligible due to the small magnitude of $V_{cb}^* V_{ub}$. In the limit that the d and s quark masses are equal, the unitarity of the CKM matrix ensures a vanishing amplitude. However, the mass difference of d and s quarks is insufficient to result in a large mixing rate. Expectations for the ratio of mixed to unmixed decay rates from the box diagram are of the order of $10^{-10} - 10^{-9}$ [2]. However, due to the smallness of the short distance contributions, long distance effects could be important. The resulting predictions for the mixing probability depend on the treatment of these effects and cover a large range, reaching values as high as 10^{-3} [3].

In direct searches, the signature of mixing is neutral D meson decay products with a charge combination opposite to that expected for a produced flavor eigenstate. Examples of appropriate $D^0 \to f$ decay modes for these methods are $D^0 \to K^-\pi^+$ and $D^0 \to K^-\ell^+\nu$[14]. If in the decay of an initially produced D^0 a $K^+\pi^-$ or $K^+\ell^-\overline{\nu}$ final state $(\overline{f})$ is observed, this represents an indication of a mixing transition $D^0 \to \overline{D}^0 \to \overline{f}$. While the semileptonic decay modes are more difficult to reconstruct due to the presence of a neutrino in the final state, the hadronic modes suffer from an irreducible background of doubly Cabibbo suppressed (DCS) decays.

To search for $D^0 - \overline{D^0}$ mixing we used the $D^{*+} \to D^0\pi_s^+, \;\; D^0 \to \overline{D^0} \to K^+e^-\overline{\nu}$ decay chain. The flavor of the produced D meson is tagged by the charge of the slow pion $(\pi_s^\pm)$ from the D^* decay. The charge of the electron determines the charm quantum number of the D meson at decay. If all the final state particles are reconstructed, signal events yield a sharp peak in the $\Delta m = m(\pi_s^+K^-e^+\nu) - m(K^-e^+\nu)$ distribution, where $m(\pi_s^+K^-e^+\nu)$ and $m(K^-e^+\nu)$ are the invariant masses of the selected particles. In order to use the Δm distribution to isolate the signal events, one needs to reconstruct the momentum of the neutrino. Since the kinematics of mixed and un-mixed decays are the same, both can be selected using the Δm observable.

Un-mixed decays, $D^{*+} \to D^0\pi_s^+, \;\; D^0 \to K^-e^+\nu$, result in the "right sign" (RS) final state charge combination, $\pi_s^+K^-e^+$. Mixed decays, $D^{*+} \to D^0\pi_s^+, \;\; D^0 \to \overline{D}^0 \to K^+e^-\overline{\nu}$, produce a "wrong sign" (WS) charge combination, $\pi_s^+K^+e^-$. Table I lists possible charge combinations of final state particles used in the analysis.

Decay	Final state	Notation
$D^{*+} \to D^0\pi_s^+, \quad D^0 \to K^-e^+\nu$, un-mixed	$\pi_s^+K^-e^+$	Right sign (RS)
$D^{*+} \to D^0\pi_s^+, \quad D^0 \to \overline{D}^0 \to K^+e^-\overline{\nu}$, mixed	$\pi_s^+K^+e^-$	Wrong sign (WS)
combinatorial background	$\pi_s^+K^\pm e^\pm$	Combinatorial sign (CS)

TABLE I: Summary of charge combinations and notations used in the analysis.

In the following section we describe the selection of D meson semileptonic decay candidates. Section 3 describes the neutrino reconstruction and calculation of Δm. A background description is presented in section 4 and the proper decay time distribution of mixed and un-mixed decays is dealt with in section 5. The succeeding section describes the fit of Δm distributions, the obtained signal yield and the time integrated mixing rate r_D. In section 7 we evaluate the systematic errors and describe several cross-checks of the measurement.

II SELECTION OF SEMILEPTONIC D DECAYS

Data set

For the present analysis, data collected by the Belle detector at the center-of-mass energy of the $\Upsilon(4S)$ resonance, corresponding to an integrated luminosity of 140 fb^{-1} were used. A detailed description of the Belle detector can be found in [4]. Simulated events were generated by the QQ generator and processed with a full simulation of the Belle detector, using the GEANT package [5]. About 410 fb^{-1} of $c\overline{c}$ quark pair Monte Carlo (MC) events were used, together with about 164 fb^{-1} light quark and about 100 fb^{-1} $B\overline{B}$ meson pair MC events, which were rescaled by the appropriate factors.

To simulate mixed D meson decays, a generic (non-mixed) MC was used with an appropriate re-weighting of the proper decay time distribution.

Selection criteria

Electron-positron interactions with hadrons in the final state are selected from data, based on the neutral cluster energy, total visible energy in the center-of-mass system (cms), z component of total cms momentum and the position of reconstructed event vertex [6], with an efficiency above 99%.

The selection criteria were optimized using the simulated sample of generic u, d, s, charm and B meson pair events, by maximizing the efficiency for non-mixed signal events multiplied by the purity of the selected sample. Since the kinematic properties of mixed and non-mixed events are the same, such an optimization ensures optimal selection for the mixed events as well.

For $\pi_s^\pm$ candidates, tracks with impact parameter with respect to the interaction point in the radial direction $|\delta r| < 1$ cm and in the beam direction $|\delta z| < 2$ cm were considered. This procedure suppressed badly reconstructed tracks and tracks which do not originate from the interaction point. A slow pion candidate was required to have a momentum of less than 600 MeV/c. To reduce the background from electrons misidentified as slow pion candidates, we required the electron identification likelihood [7] for each track, based on the

information from the central drift chamber, aerogel Cherenkov counter and electromagnetic calorimeter, to be lower than 0.1. To illustrate the $\pi_s^{\pm}$ selection criteria the MC efficiency for reconstruction of a slow pion track was found to be around 60%. Electron candidates were required to have a momentum $p > 600$ MeV/c and an electron identification likelihood [7] above 0.95. By that 45% of all simulated signal electrons are reconstructed. From the remaining tracks in an event, charged kaon candidates were chosen with momentum above 800 MeV/c. Using the information from the time of flight counters, central drift chamber and aerogel Cherenkov counters, a relative likelihood $\mathcal{L}$ for a given track to be a $K^{\pm}$ or $\pi^{\pm}$ is obtained [6]. Kaon candidates were selected using $\mathcal{L}(K^{\pm})/(\mathcal{L}(K^{\pm})+\mathcal{L}(\pi^{\pm})) > 0.5$. Using this selection about 50% of signal kaons were retained.

In order to reduce the combinatorial background and the background from $B\overline{B}$ events, and to improve the resolution in the Δm, a requirement for the cms momentum of the kaon-electron system, $p^*(Ke) > 2$ GeV/c was imposed. To further suppress D^0 mesons arising from $B\overline{B}$ events, we required the ratio of the second and zeroth Fox-Wolfram moments R_2 to be greater than 0.2 [8].

Background from $D^0 \to K^-\pi^+$, with π^+ misidentified as e^+ (RS sample) or with K^- misidentified as e^- and π^+ as K^+ (WS sample), was suppressed using a requirement on the invariant mass of the $K-e$ system, $M(Ke) < 1.82$ GeV/c^2. Another source of background contributing to the RS and WS samples is the $D^0 \to K^-K^+$ decay with either of the charged kaons misidentified as an electron. This background is effectively suppressed by the requirement $|M(KK) - m_{D^0}| > 10$ MeV/c^2, where $M(KK)$ is the invariant mass of the kaon and electron candidate, calculated using the kaon mass for both tracks.

An important source of background are the electrons from photon conversions, which could be selected as electron or slow pion candidates. Combinations where both π_s^+ and e^- candidates are from conversions, are almost completely suppressed by requiring $M(e^+e^-) <$ 150 MeV/c^2, where the electron mass is assigned to the π_s^+ candidate. A further search for an additional $e^{\pm}$ of opposite charge as the semileptonic electron candidate or as the slow pion candidate was performed in each event. Again, events with $M(e^+e^-)$ below 150 MeV/c^2 were rejected. For the events satisfying all the above criteria, the neutrino reconstruction was performed.

III NEUTRINO RECONSTRUCTION

Four-momentum conservation in an e^+e^- collision implies

$$P_\nu = P_{\mathrm{cms}} - P_{\pi_s Ke} - P_{\mathrm{rest}} \tag{2}$$

for the signal decay, where cms stands for the center-of-mass four-momentum of the e^+e^- system, and the index *rest* indicates the four-momentum of all detected particles except the slow pion, charged kaon and the electron candidate[15]. The variable P_{rest} is calculated using all the remaining charged tracks in the event with $|\delta r| < 1$ cm and $|\delta z| < 2$ cm and all photons with energies above 100 MeV. A first approximation for the neutrino four-momentum P_ν is obtained using Eq. 2. The resulting $\Delta m = M(\pi_{\mathrm{s}}^+K^-e^+\nu) - M(K^-e^+\nu)$ distribution for signal events is shown in Fig. 2a as the dashed histogram. It has a peak at 0.145 GeV/c^2, the $D^{*\pm} - D^0$ mass difference, and with a full width at half maximum (FWHM) of 55 MeV/c^2.

Two kinematic constraints were used to improve the resolution on the neutrino momentum. First, the square of the invariant mass of selected particles was calculated using

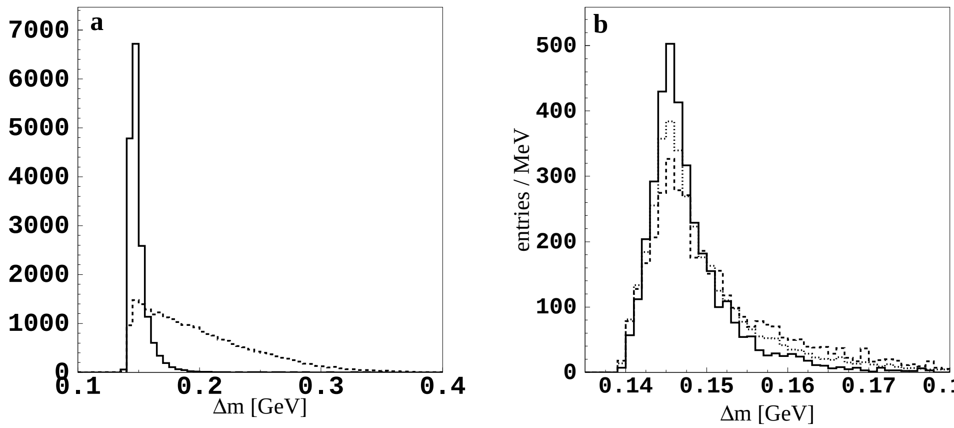

FIG. 2: a) Δm distribution for simulated signal events using the missing momentum for neutrino reconstruction (dashed histogram) or the missing momentum together with the constraints on the missing mass and the mass of the D^{*+} (solid histogram) as described in the text. b) Δm distribution for simulated signal events in different bins of the momentum of the kaon-electron system: $p^*(Ke) < 2.0$ GeV/c (dashed histogram), 2.0 GeV/c $< p^*(Ke) < 3.2$ GeV/c (dotted histogram), 3.2 GeV/c $< p^*(Ke)$ (solid histogram). The histograms are normalized to the same area.

$M^2(\pi_s K e\nu) = (P_\nu + P_{\pi_s Ke})^2$. For signal events the invariant mass should equal the mass of the $D^{*\pm}$ meson, $m_{D^{*\pm}}$. Only events with -4 GeV/c^2 $< M(\pi_s K e\nu)^2 < 36$ GeV/c^2 were retained. For the selected events, the magnitude of $P_{\rm rest}$ was rescaled by a factor x requiring

$$M(\pi_s K e\nu)^2 = (P_{\rm cms} - x \cdot P_{\rm rest})^2 \equiv m_{D^{*\pm}} \ , \tag{3}$$

with $m_{D^{*\pm}}$ fixed to the nominal value of 2.010 GeV/c^2 [9].

As a second kinematic constraint, the square of the missing mass, P_ν^2, is used. For events satisfying -2 GeV/c^2 $< P_\nu^2 < 0.5$ GeV/c^2, the angle α between the direction of $\vec{p}_{rest}$ and the direction of the $\pi_s Ke$ system momentum was corrected in order to yield

$$m_\nu^2 = (E_{\rm cms} - E_{\pi_s Ke} - E_{\rm rest})^2 - p_{\pi_s Ke}^2 - p_{\rm rest}^2 - 2 p_{\pi_s Ke} p_{\rm rest} \cos\alpha \equiv 0. \tag{4}$$

The angle α was corrected by rotating $\vec{p}_{rest}$ in the plane determined by the vectors $\vec{p}_{rest}$ and $\vec{p}_{\pi_s Ke}$.

The Δm distribution obtained using the neutrino four-momentum after the use of kinematic constraints is shown in Fig. 2a as the solid histogram. The resolution is significantly improved, with the FWHM being about 7 MeV/c^2. It also improves at higher values of $p^*(Ke)$, as illustrated in Fig. 2b. Using the simulated background events it has been verified that the described neutrino reconstruction does not induce any peaking in the background Δm distribution.

The MC prediction for the reconstructed Δm distribution is shown in Fig.3; the fraction of signal events in the $\Delta m < 0.18$ GeV/c^2 region is $f_s = 0.620 \pm 0.001$. The background is composed of $(75.6 \pm 0.2)\%$ $c\overline{c}$ events, $(5.4 \pm 0.1)\%$ light quark events and $(18.9 \pm 0.1)\%$ $B\overline{B}$ events. There is a small fraction (about 1%) of signal events arising from $B\overline{B}$ events. At this stage the efficiency for reconstructing the signal with $\Delta m < 0.18$ GeV/c^2 is found to be $(5.4 \pm 0.1)\%$.

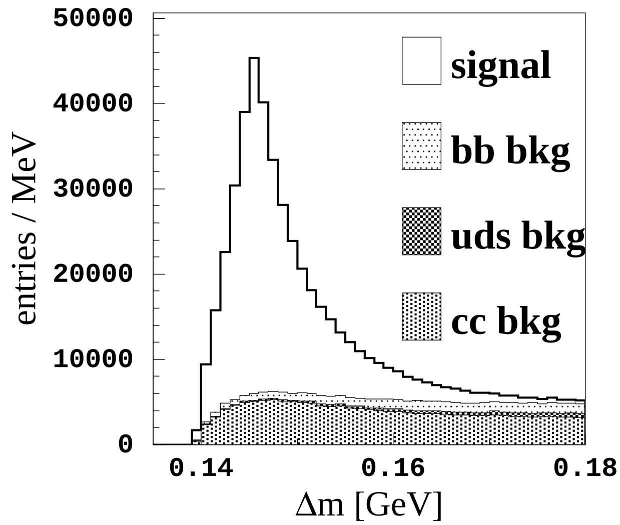

FIG. 3: Simulated distribution for Δm with neutrino momentum reconstruction using kinematic constraints. The open histogram shows the contribution of the signal and the hatched histograms show individual contributions to the background.

IV BACKGROUND EVALUATION AND Δm DISTRIBUTION

Background in the RS sample

To check the MC and to avoid systematic errors arising from a possible discrepancy with the data, the majority of the background was described using the data. The combinatorial, charge un-correlated background in the RS Δm distribution can be described using "combinatorial sign" (CS) track combinations (Table I). These are composed of a slow pion candidate, $\pi_s^{\pm}$, and a kaon and electron of the same charge, $K^{\pm}e^{\pm}$. Since such combinations cannot arise from semileptonic decays of D mesons, they describe random track combinations giving rise to a background with a Δm value less than 0.18 GeV/c^2. Fig. 4a shows a comparison of Δm for all MC RS background events and CS data events; the former shows an excess of events in the region of low Δm. This is a consequence of the charge-correlated track combinations apart from the signal itself, present in the RS sample.

There are additional semileptonic decays with the same charge combination of final state charged tracks as in the $D^0 \to K^- e^+ \nu$ decay. The most important one is $D^0 \to K^- e^+ \nu \pi^0$, which according to the simulation represents [16] 8.8% of all reconstructed events with $\Delta m <$ 0.18 GeV/c^2. Other modes, like Cabibbo suppressed $D^0 \to \pi^- e^+ \nu$, or $D^0 \to \pi^- e^+ \nu \overline{K}^0$ decays, with a charged pion misidentified as a kaon[16], represent an additional 1% of simulated events in Fig. 4a. The charge correlation is also preserved if the slow pion decays into a muon, and the latter is taken as a slow pion candidate (0.7% of all reconstructed events).

These decay channels have two important properties: they tend to peak at low values of Δm and secondly, the charge of the kaon or electron candidate, together with the charge of the slow pion from a D^{*+} decay, carries the same information on possible mixing as in the

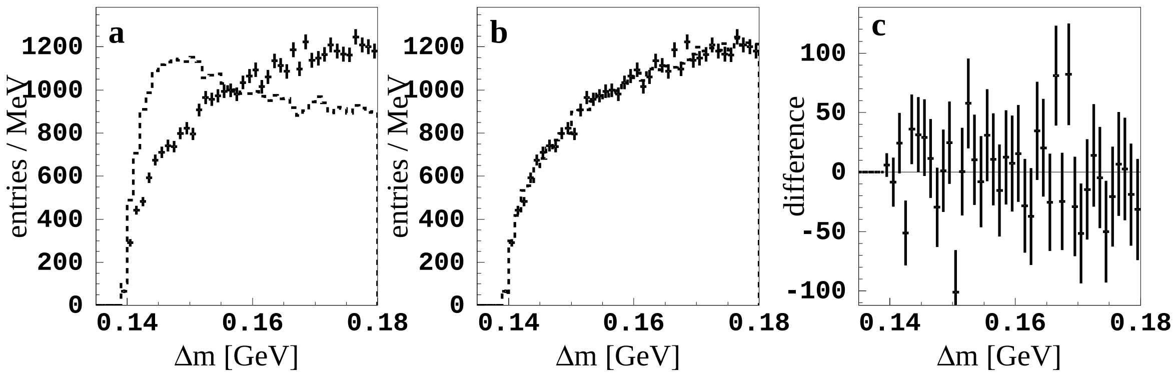

FIG. 4: a) Δm distribution for all simulated RS background events (dashed histogram) and for CS data events (points with error bars). Histograms are normalized to the same number of entries. b) The same comparison after associated signal and $D^0 \to K^-\pi^+\pi^0$ decays are removed from the simulated RS distribution. c) The difference between the normalized Δm distributions for CS data and the remaining simulated RS background.

case of the selected signal decay. In the following, these decays are treated as a part of the signal and described as *associated signal*.

Apart from the processes included in the signal, there are a number of hadronic D^0 decays and decays where particle misidentification might appear, contributing to a charge-correlated background. Using measured branching ratios for the individual processes [9], measured and simulated average misidentification rates and estimates of corresponding CKM elements for the DCS decays, we find that the most important contribution to the charge-correlated background in the RS sample is the decay $D^0 \to K^-\pi^+\pi^0$. This is confirmed using the MC. Contributions from other decays are expected to be almost an order of magnitude smaller. The Δm distribution and the amount of the charge correlated background were evaluated using the MC sample. The hadronic background accounts for $0.44 \pm 0.01\%$ of all events with $\Delta m \leq 0.18$ GeV/c^2 and is included in the CS Δm distribution when extracting the yield of RS events.

After removing the associated signal processes and the contribution from $D^0 \to K^-\pi^+\pi^0$ decays from the simulated RS background, the agreement of the Δm distribution with the CS data is good. The comparison is shown in Fig. 4b and c. The χ^2, calculated from the difference of the two, has a value of 36.5 for 40 degrees of freedom.

Background in the WS sample

While the CS events represent a good description of the combinatorial background for the RS sample, the shape of the WS sample combinatorial background is different (Fig. 5a). This is due to different fractions of events, where the slow pion candidate is a true $\pi_s^\pm$ from a $D^{*\pm}$ decay and either the kaon or electron candidate (or both, at least one being misidentified) are from the corresponding D^0 decay. The amount of this background, which will be referred to as the *angularly correlated* background, is much smaller in the WS sample. The rest of the background is angularly uncorrelated and represents the majority of the background

in the WS sample. Therefore WS background events were described by combining a D^0 candidate from one event with a slow pion candidate from another event (*embedded pions*). The shape of the Δm distribution using the embedded pions agrees well with the MC predicted angularly uncorrelated WS background distribution. The comparison is shown in Fig. 5b and 5c. The χ^2 of the difference was found to be 33.1 for 40 d.o.f. An additional $(2.04 \pm 0.05)\%$ of angularly correlated background is not represented by using embedded $\pi_s^{\pm}$. The MC simulation shows that the largest contribution to this background comes from $D^0 \to K^-\pi^+\pi^0$, as already established for the RS sample. The Δm distribution for these events was obtained from simulation and added to the background described by the embedded slow pions.

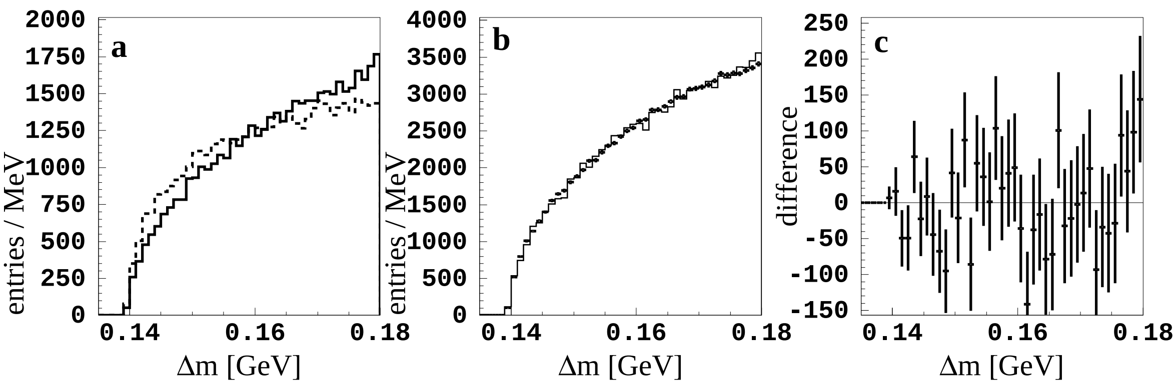

FIG. 5: a) Simulated Δm distribution for WS (solid histogram) and RS (dashed histogram) backgrounds. Both are normalized to the same area. b) Comparison of simulated WS background without the contribution of angularly correlated background (solid histogram) with the background obtained using the embedded pions (points with error bars). c) The difference of the two (normalized) distributions shown in the previous plot.

A preliminary binned χ^2 fit to the Δm distribution of RS data events was performed, before any proper decay time selection. For the signal and associated signal the simulated shape of Δm, $P_s(\Delta m)$, was assumed. Background in this sample was described using the CS data events with an additional contribution from $D^0 \to K^-\pi^+\pi^0$ events, $P_b^R(\Delta m)$. The fraction of the latter was fixed in the fit to the value predicted by the MC. The data distribution was fitted with

$$\mathcal{P}_R(\Delta m) = \mathcal{N}_R(f_s^R P_s(\Delta m) + (1 - f_s^R)P_b^R(\Delta m)) \quad , \tag{5}$$

where the fraction of signal events (including the associated signal) f_s^R and an overall normalization $\mathcal{N}_R$ were the free parameters. The result of the fit was $f_s^R = 0.732 \pm 0.003$.

In order to enhance the sensitivity to mixed D^0 decays a selection based on the proper decay time was used, as explained in the next section.

V PROPER DECAY TIME DISTRIBUTIONS

It should be noted that in the present analysis no attempt is made to obtain results on the mixing rate from the fit to proper decay time distributions of D^0 mesons. The decay time

is used only to select possible mixed decays with a higher purity. To measure the mixing rate from the ratio of WS and RS events, one needs to evaluate the ratio of acceptances for mixed and non-mixed decays for decay times larger than a chosen value. The purpose of this section is to describe the estimation of the acceptance ratio, in which most of the systematic uncertainties cancel.

The mixed events are expected to have the following proper decay time distribution [10]:

$$\mathcal{P}_{\rm WS}(t') \propto t'^2 \; e^{-t'/\tau_{D^0}} \;, \qquad (6)$$

with $\tau_{D^0} = (411.7 \pm 2.7) \times 10^{-15}$ s [9] denoting the lifetime of neutral D mesons. The sensitivity to mixed events can be enhanced by selecting D^0 decays with a longer proper decay time, as the background events tend to be concentrated at lower decay times. The decay time t' is evaluated using the decay length from the e^+e^- interaction point to the reconstructed D^0 decay vertex, and the measured momentum of the meson; due to the shape of the KEK-B accelerator interaction region, which is narrowest in the vertical (y) direction, the dimensionless proper decay time t is calculated as

$$t = \frac{t'}{\tau_{D^0}} = \frac{m_{D^0}}{p_y} \; \frac{y_{\rm vtx} - y_{\rm IP}}{c\tau_{D^0}} \; . \qquad (7)$$

p_y is the y component of the D^0 candidate's momentum and $y_{\rm vtx}$ and $y_{\rm IP}$ are the y coordinates of the reconstructed $K - e$ vertex and of the interaction point, respectively. The observed t distribution is smeared due to the experimental resolution. Fig. 6a shows the decay time distribution of RS data events with $\Delta m < 0.18$ GeV/c^2.

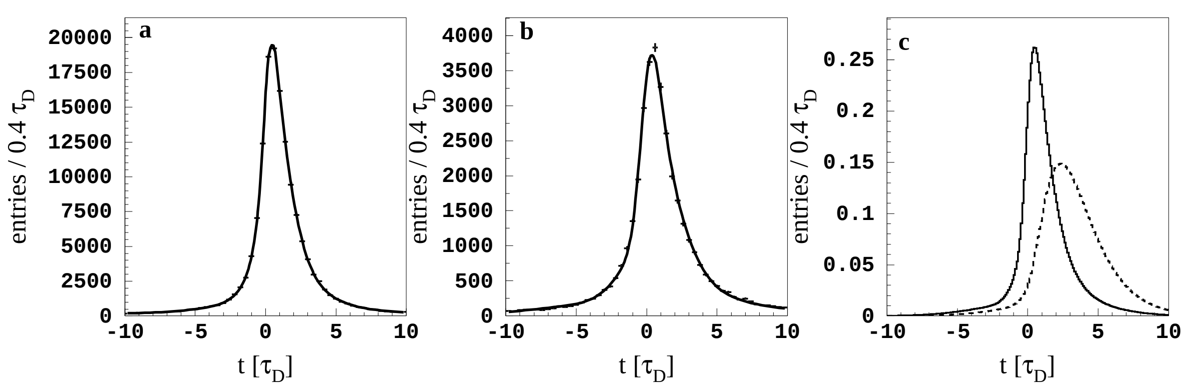

FIG. 6: a) Measured proper decay time distribution for the RS events (points with error bars). The solid line shows the results of the fit described in the text. b) Distribution of WS background events, obtained by combining a D^0 candidate with an embedded $\pi_s^\pm$. The solid line is again a the result of the fit described in the text. c) Expected decay time distribution of $D^0 \to K^- e^+ \nu$ decays (solid line) and $D^0 \to \overline{D^0} \to K^+ e^- \overline{\nu}$ (dashed line) calculated using the parameters obtained from the fit to the RS event time distribution.

We fit the RS decay time distribution with a signal and a background term. The former is an exponential convolved with a sum of three Gaussians, describing the detector resolution. The background contribution is composed of a lifetime (exponential) and a prompt (delta function) component, convolved with the resolution function. The resulting value of the

mean t for the signal part is 1.093 ± 0.044. A similar fit is performed on the WS background events (Fig. 6b), using the same ansatz as for the RS background. From the fitted parameters we deduce the expected decay time distribution of un-mixed and mixed decays, shown in Fig. 6c. To improve the sensitivity to mixed decays, we compare the expected decay time distribution of mixed decays with that for background (Fig.6b). The optimum for the selection criterion is found to be $t > 1.5$. This requirement is imposed on both RS and WS events. By doing that, the final ratio of WS and RS signal events depends only on the ratio of decay time selection efficiencies for the two classes of events, $\epsilon^{\rm unmix}/\epsilon^{\rm mix}$. Taking the ratio of efficiencies instead of applying the described selection to WS events only reduces the systematic error arising from an imperfect description of the decay time distributions. For the ratio of efficiencies for $t > 1.5$ we obtain $\epsilon^{\rm unmix}/\epsilon^{\rm mix} = 0.420 \pm 0.010$, where the error is obtained by varying all the parameters of the fit to decay time distributions by one standard deviation.

Table II shows the composition of the simulated sample after the proper decay time selection.

Component	Fraction [%]	Component	Fraction [%]
RS		WS	
signal	57.7 ± 0.1	$c\overline{c}$ bckg.	73.6 ± 0.1
assoc. signal	12.4 ± 0.1	angularly corr. bckg.	2.18 ± 0.08
$c\overline{c}$ bckg.	21.9 ± 0.1	uds bckg.	12.9 ± 0.1
$D^0 \to K^-\pi^+\pi^0$	0.55 ± 0.02	$B\overline{B}$ bckg.	13.5 ± 0.1
uds bckg.	2.63 ± 0.06		
$B\overline{B}$ bckg.	4.9 ± 0.1		

TABLE II: Composition of the simulated selected samples. The indented contributions are sub-samples of the above component. The quoted errors on the fractions are due to the MC statistics only.

VI FIT OF Δm DISTRIBUTION

Signal yield

The Δm distributions for RS and WS events, after all selection requirements, including $t > 1.5$, are shown in Fig. 7.

The data distributions are fitted using a binned χ^2 fit. The RS distribution is described as explained in section 4. In the fit we minimize the value of

$$\chi^2 = \sum_{i=1}^{N_{\rm bin}} \frac{(N_i - \mathcal{P}_R(\Delta m_i))^2}{\sigma^2(N_i) + \sigma^2(\mathcal{P}_R(\Delta m_i))} \quad . \tag{8}$$

N_i is the number of entries in the i-th bin of the RS data distribution and $\mathcal{P}_R(\Delta m_i)$ is given by the number of entries of MC signal, CS and simulated $D^0 \to K^-\pi^+\pi^0$ events in this bin. Both errors, on N_i and on $\mathcal{P}_R(\Delta m_i)$, are included in the χ^2 definition.

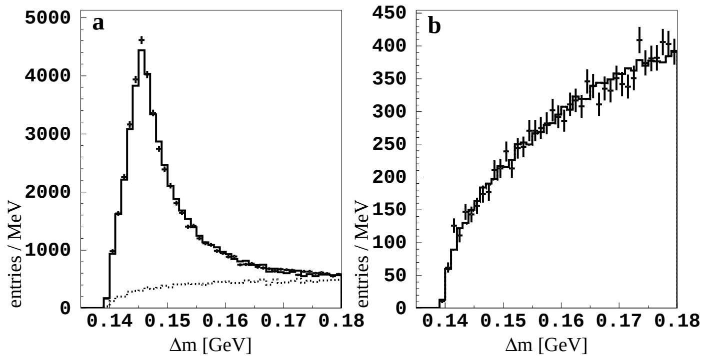

FIG. 7: a) Distribution of Δm for RS events. b) Distribution of Δm for WS events. Data is shown with error bars, the solid histogram shows the fit, as explained in the text. The background contribution is shown as the dashed histogram.

From the fitted values of f_s^R (signal fraction) and $\mathcal{N}_R$ (overall normalization) we obtain the number of signal non-mixed events $N_{\rm RS} = 40198 \pm 329$. The quoted error includes the statistical error of the data as well as the error due to the limited statistics of the expected distributions (the same holds for the fit to the WS sample, described below). The χ^2 of the fit with 39 degrees of freedom is 69.5. The goodness-of-fit depends strongly on the amount of the associated signal included, due to the different widths for the Δm distributions of $D^0 \to K^- e^+ \nu$ and associated decay modes. This contribution is treated as one of the sources of the systematic uncertainty.

For the WS sample the same description of the signal ($P_s(\Delta m)$) as for the RS sample is used, while the background ($P_b^W(\Delta m)$) is described using the embedded slow pions with the addition of simulated angularly correlated background. The result of the fit with

$$\mathcal{P}_W(\Delta m) = \mathcal{N}_W(f_s^W P_s(\Delta m) + (1 - f_s^W) P_b^W(\Delta m)) \tag{9}$$

is $f_s^W = (1.7 \pm 6.0) \times 10^{-3}$. The quality of the fit is good: $\chi^2 = 37.9$ for 39 degrees of freedom. The number of mixed events obtained by the fit is $N_{\rm WS} = 19 \pm 67$.

Time integrated mixing rate

The time integrated mixing rate r_D is defined as [9]

$$r_D = \frac{\int_0^\infty \mathcal{P}(D^0 \to \overline{D}^0 \to \ell^- X^+, t)}{\int_0^\infty \mathcal{P}(D^0 \to \ell^+ X^-, t)} \approx \frac{x^2 + y^2}{2} \quad , \tag{10}$$

where the time dependent probabilities for un-mixed and mixed events are taken to be of the form $e^{-t/\tau}$ and $t^2 e^{-t/\tau}$, respectively. The dimensionless mixing parameters x and y are equal to $x = \Delta M/\Gamma$ and $y = \Delta\Gamma/2\Gamma$, where ΔM is the mass difference of the two neutral D meson mass eigenstates, $\Delta\Gamma$ is the difference of the decay widths and Γ is the average decay width of the two.

The parameter r_D is obtained from the fitted WS and RS yields,

$$r_D = \frac{N_{\rm WS}}{N_{\rm RS}} \cdot \frac{\epsilon^{\rm unmix}}{\epsilon^{\rm mix}} \quad , \tag{11}$$

with the ratio of efficiencies for decay time selection given in Section 5. The result is

$$r_D = (0.20 \pm 0.70) \times 10^{-3} \quad , \tag{12}$$

where the quoted uncertainty is statistical only.

VII SYSTEMATIC UNCERTAINTIES

Estimation of systematic errors

The value of the time integrated mixing rate is obtained using the ratio of WS and RS D^0 decays. Since the kinematics of these decays is the same, the selection efficiencies, excluding the acceptance of the proper decay time selection, are expected to be the same for both types of decays and hence cancel in the final expression (11). Using the MC sample of events we find the selection efficiency ratio to be 0.97 ± 0.05, compatible with this expectation.

The influence of the kinematic constraints in the neutrino reconstruction on the Δm distribution of background has been verified using the MC simulation and no artificial peaking has been observed. The fit to the RS sample Δm distribution correctly reproduces the number of signal events. For the simulated value of $N_{\rm RS}^{\rm in} = 59561$ we obtain $N_{\rm RS}^{\rm out} = 59193 \pm 498$. Although the numbers of RS events agree within the statistical error of the fit, the remaining relative difference is propagated to an absolute error on r_D of 0.001×10^{-3} and is added to the total systematic error. The reconstruction of WS events has also been verified using the simulated sample. To a sample of 2.93×10^6 non-mixed events, roughly corresponding to an integrated luminosity of 180 fb^{-1}, we added 6000 mixed D meson decays, obtaining a sample of D^0 decays with an input value of $r_D^{GEN} = 2.05 \times 10^{-3}$. The fit (Fig. 8) with the same method as used for the data yields $N_{\rm WS}^{\rm out} = 234 \pm 85$ and $N_{RS} = 48459 \pm 420$. The former can be compared to the simulated value of $N_{\rm WS}^{\rm in} = 255$. The fitted numbers of signal events result in $r_D = (2.0 \pm 0.7) \times 10^{-3}$, which very well reproduces the input value. Here also the relative difference between the simulated and reconstructed $N_{\rm WS}$ is taken into account in the final systematic error.

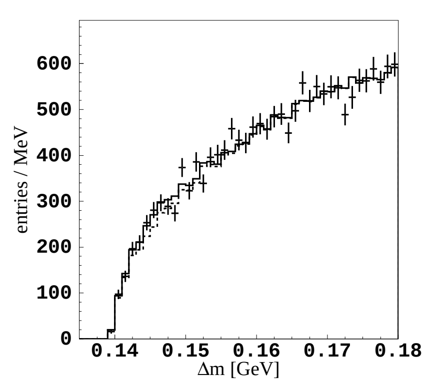

FIG. 8: Distribution of Δm for simulated events including mixed D mesons (points with error bars), the fit (solid line) and the background (dashed line).

The error on the ratio of decay time selection efficiencies $\epsilon^{\rm unmix}/\epsilon^{\rm mix}$ is obtained by varying the fitted parameters of the RS and WS sample proper decay time distributions and leads

to an additional 0.005×10^{-3} error on r_D. We evaluated the same efficiency ratio using the MC sample and obtained $\epsilon^{\text{unmix}}/\epsilon^{\text{mix}} = 0.400 \pm 0.012$, which is consistent with the value obtained from the proper decay time fit. The proper decay time selection was additionally verified by performing the fit to RS and WS Δm distributions using several different decay time requirements, $t > 1.2$ and $t > 1.7$. The resulting values of r_D are $(0.30 \pm 0.70) \times 10^{-3}$ and $(0.21 \pm 0.70) \times 10^{-3}$, respectively. We take the largest difference as a systematic error due to an imperfect description of the decay time distribution.

The next possible source of systematic uncertainty arises from MC samples used to fit the Δm distributions. Using the measured branching fractions and corresponding errors [9] of decay channels included in the associated signal, and their relative contributions to the selected sample as obtained by MC, we estimate that the amount of this component in the fit needs to be varied by 40%. The fit was repeated and the difference in the obtained values of r_D is found to be 0.015×10^{-3}.

The fraction of the angularly correlated WS background is estimated from MC to be $(2.04 \pm 0.05)\%$. Since the majority of these events arise from $D^0 \to K^-\pi^+\pi^0$ decays, we repeated the WS fit by changing the amount of this background in accordance with the relative error on $B(D^0 \to K^-\pi^+\pi^0)$ [9]. The variation of N_{WS} resulted in a 0.05×10^{-3} error on r_D.

The systematic uncertainties are summarized in Table III. By summing the individual contributions in quadrature, we obtain the total systematic error of 0.11×10^{-3}. It is clear that the uncertainty of the result on the time integrated mixing rate is limited by the statistics of the data.

Source	Estimated by	Resulting r_D uncertainty [$\times 10^3$]
ν reconstruction	$\lvert N_{\text{RS}}^{\text{in}} - N_{\text{RS}}^{\text{out}} \rvert / N_{\text{RS}}^{\text{in}}$	± 0.001
	$\lvert N_{\text{WS}}^{\text{in}} - N_{\text{WS}}^{\text{out}} \rvert / N_{\text{WS}}^{\text{in}}$	± 0.016
ratio of t selection	$\pm 1\sigma$ of t distribution fit parameters	± 0.005
efficiencies	using different t selection values	± 0.100
amount of associated signal	$\pm 40\%$	± 0.015
amount of charge correlated WS backg. ($D^0 \to K^-\pi^+\pi^0$)	$\pm 7\%$	± 0.050
Total		± 0.11

TABLE III: Summary of systematic measurement uncertainties. The evaluation of individual contributions are described in the text.

Checks of the analysis method

Apart from the checks on the quality of background description described in previous sections, several other tests of the analysis method were performed.

The fits to the RS Δm distribution were done individually for different data taking periods. The resulting signal fractions show no significant deviation from the overall result used in the analysis.

In order to check for a possible bias in the result, we performed a fit to the Δm distribution of WS events using an inverted decay time selection, i.e. fitting the events with $t < 1.5$. A

possible mis-assignment of the charge of the slow pion candidate, for example, would appear as a peak in this sample and could bias the fitted number of WS events. Since $t < 1.5$ is the region where the sensitivity to mixed events is reduced, we expect no such contribution and any positive signal would be an indication of a peaking background behavior. The fit was done in the same manner as the fit to $t > 1.5$ distribution and the resulting number of mixed events is $N_{\rm WS} = -77 \pm 88$, in accordance with the expectation. The fitted number of non-mixed decays is $N_{\rm RS} = 82943 \pm 456$, which taking into account the corresponding ratio of decay time selection efficiencies gives $r_D = (-3.1 \pm 3.6) \times 10^{-3}$.

By repeating the fit procedure without the decay time selection, we obtain $N_{\rm WS} = -48 \pm 111$ and $N_{\rm RS} = 123054 \pm 562$. While the central value of $r_D = (-0.39 \pm 0.90) \times 10^{-3}$ is compatible with the null result, as for the events with $t > 1.5$, the statistical error is increased, confirming the usefulness of the decay time selection.

To test the bias as well as the obtained statistical error of $N_{\rm WS}$ we divided the available simulated WS sample into two parts. The corresponding Δm distributions were then fitted one to another. The result of the fit is $N_{\rm WS} = -66 \pm 62$. The statistical error of the "background" distribution was not included in this fit. Afterward we independently varied the contents of each bin within the statistical error and repeated the fit many times. The distribution of resulting $N_{\rm WS}$ is centered at the starting value (due to a statistical fluctuation when arbitrarily dividing the MC sample into two parts) with a width of 61.9 ± 0.5. The latter represents the expected statistical error of the fit on a sample with about the same statistics as the data itself. The expected error is in agreement with the fit to the data when not taking into consideration the statistical error of the expected distributions (± 64).

VII CONCLUSIONS

We have searched for $D^0 - \overline{D^0}$ mixing in semileptonic D meson decays. The resulting time integrated mixing rate is

$$r_D = (0.20 \pm 0.70 \pm 0.11) \times 10^{-3} \quad , \tag{13}$$

where the first error represents the statistical and the second the systematic uncertainty.

Since no significant signal for the WS decays $D^0 \to K^+ e^- \nu$ is observed, we put an upper limit on the time integrated mixing rate. We combine statistical and systematic errors in quadrature and asume a Gaussian distribution of the resulting total error; using the Feldman Cousins approach[13] to estimate the upper limit in the vicinity of the physical boundary ($r_D \geq 0$) we find

$$r_D \leq 1.4 \times 10^{-3} \ \text{ at } 90\% \text{ C.L.} \tag{14}$$

The limit obtained is more restrictive than the existing world average $\Gamma(K^+\ell^-\overline{\nu})/\Gamma(K^-\ell^+\nu) < 5 \times 10^{-3}$[9]. Using expression (10) and the value of $\Delta\Gamma/\Gamma = 2y = 0.016 \pm 0.010$[9], the above result can be expressed as

$$\Delta M \leq 13 \times 10^{10} \ \hbar s^{-1} \ \text{ at } 90\% \text{ C.L.} \tag{15}$$

Acknowledgments

We thank the KEKB group for the excellent operation of the accelerator, the KEK Cryogenics group for the efficient operation of the solenoid, and the KEK computer group

and the National Institute of Informatics for valuable computing and Super-SINET network support. We acknowledge support from the Ministry of Education, Culture, Sports, Science, and Technology of Japan and the Japan Society for the Promotion of Science; the Australian Research Council and the Australian Department of Education, Science and Training; the National Science Foundation of China under contract No. 10175071; the Department of Science and Technology of India; the BK21 program of the Ministry of Education of Korea and the CHEP SRC program of the Korea Science and Engineering Foundation; the Polish State Committee for Scientific Research under contract No. 2P03B 01324; the Ministry of Science and Technology of the Russian Federation; the Ministry of Education, Science and Sport of the Republic of Slovenia; the National Science Council and the Ministry of Education of Taiwan; and the U.S. Department of Energy.

---

* on leave from Nova Gorica Polytechnic, Nova Gorica

[1] M. Kobayashi and T. Maskawa, Prog. Theor. Phys. **49**(1973) 652; N. Cabibbo, Phys. Rev. Lett. **10**(1963) 531.

[2] H. Y. Cheng, Phys. Rev. **D 26**(1982) 143; A. Datta, D. Kumbhakar, Zeit. Phys. **C27**(1985) 515.

[3] L. Wolfenstein, Phys. Lett. **B 164**(1985) 170; J. Donoghue et al., Phys. Rev. **D 33**(1986) 179; H. Georgi, Phys. Lett.**B297**(1992) 353; T. Ohl et al., Nucl. Phys. **B403**(1993) 605.

[4] A. Abashian *et al.*, Belle Collab., Nucl. Instr. Meth. **A 479**(2002) 117.

[5] Events are generated with the CLEO QQ generator (see http://www.lns.cornell.edu/public/CLEO/soft/QQ); the detector response is simulated with GEANT, R. Brun *et al.*, GEANT 3.21, CERN Report DD/EE/84-1, 1984.

[6] K. Abe *et al.*, Belle Collab., Phys. Rev. **D66**(2002) 032007.

[7] K. Hanagaki *et al.*, Nucl. Instrum. Meth. **A 485**(2002) 490.

[8] G. C. Fox, S. Wolfram, Phys. Rev. Lett. **41**(1978), 1581.

[9] K. Hagiwara *et al.*, Phys. Rev. **D66**(2002) 010001.

[10] See for example Zhi-zhong Xing, Phys. Rev. **D55**(1997) 196.

[11] L. Gladilin, hep-ex/9912064.

[12] D. Bortoletto *et al.*, Cleo Collab., Phys. Rev. **D37** (1988) 1719.

[13] G. J. Feldman, R. D. Cousins, Phys. Rev. **D57**, 3873 (1998).

[14] Throughout the paper charge conjugated modes are implied unless stated otherwise.

[15] In the following, P denotes the particle's 4-momentum while $\vec{p}$ and p denote the 3-dimensional momentum and its magnitude, respectively.

[16] This includes the $D^0 \to K^{*-}e^+\nu$ decay mode.